Available online at www.sciencedirect.com
ScienceDirect
Materials and Design xxx (2006) xxx–xxx
Materials & Design
www.elsevier.com/locate/matdes

The effects of static, dynamic and fatigue behavior on three-dimensional shape optimization of hip prosthesis by finite element method

Oguz Kayabasi *, Bulent Ekici

Department of Design and Manufacturing Engineering, Gebze Institute of Technology, PK. 141, 41400 Gebze/Kocaeli, Turkey
Department of Mechanical Engineering, University of Marmara Kuyubasi/Goztepe, 81040 Istanbul, Turkey

Received 15 February 2006; accepted 14 August 2006

Abstract

The finite element method, one of the most advanced simulation techniques in solid mechanics, is used for orthopedic biomechanics. It is used as a tool for the design and analysis of total joint replacement and other orthopedic devices. The design of hip joint prostheses is a complex process that requires close co-operation between engineers and surgeons. To design highly durable prostheses one has to take into account the natural processes occurring in the bone. One of the most important factors in the implant design is to reduce stress on the femur and the bone-cement. The purpose of this study is to investigate the behavior of newly designed implants under body weight load during stumbling by parametric modeling. Two different implant materials have been selected to study appropriate material and fatigue life resistant. In the parametric design, the prosthesis functional requirement is that the locking of stem to the femur head using cement should be strong enough to preclude unlocking during the life time of a patient and to prevent sliding of the implant into the bone-cement.

In the finite element analysis, physical interactions among joints are simulated by contact algorithms. The femur–bone-cement interface and the bone-cement–implant interface surface to surface contact algorithms of ANSYS were used for implicit static analysis. Three stem-cement interface conditions are considered: completely bonded, debonded with coefficient of friction 0, and debonded with coefficient of friction 0.2. In the analysis, a viscoelastic material model is utilized for bone-cement. Numerical shape optimization is applied to the prosthesis.

The results of finite element simulations are compared with Charnley's implant results and appropriate material for the implant is proposed. The best stem shapes fulfilling the desired functional requirements are chosen for the design. These findings can form a base for further research such as the optimum design of bone-implant hip prosthesis.
© 2006 Published by Elsevier Ltd.

Keywords: Optimization; Fatigue; Finite element method; Hip prosthesis

1. Introduction

Orthopedic implants are intended to support forces and must thereby be firmly attached to the rest of the skeleton [1]. The implant is placed in the body either with an acrylic cement that gradually fails as regeneration of connecting bone tissue is proceeding, or without cement using an implant with an interface designed to provide the necessary attachment. Cemented implant is still used in the majority of operations.

Conventional design and analysis of bone-implant hip prosthesis rely on expert's knowledge, experience and ability to avoid any irreversible damage on the bones of patients. Because of the difficulty of performing implant tests in vivo, mathematical models have been developed to carry out the structural analysis of implants before application on a patient. Accordingly bone-implant hip prosthesis could be designed and studied with computer simulations. The finite element method (FEM) is an advanced simulation technique that has been used in orthopedic biomechanics since 1972 [2]. It is an important tool used in the design and analysis of total joint replacements and other orthopedic

* Corresponding author. Tel.: +90 262 653 8497; fax: +90 262 653 8490.
E-mail address: oguzk@gyte.edu.tr (O. Kayabasi).

0261-3069/$ - see front matter © 2006 Published by Elsevier Ltd.
doi:10.1016/j.matdes.2006.08.012

devices. FEM modeling and analysis present a non-destructive design approach for bone-implant hip prosthesis. It allows many what-if scenarios to be studied in computer environment before the prosthesis is actually inserted. This simulation streamlines the design and prevents any permanent damage caused by mis-implementation.

Performance and success of long-term survival of cemented Total Hip Arthroplasty (THA) is an attachment of the prosthesis to the bone. Cement–metal interface failures of separation of the stem-cement interface and fractures in the cement may initiate the initial loss of the fixation of the implant [3]. Particularly, interface debonding and cement fatigue failure are now likely to cause long-term loosing of the implant, leading to damage accumulation failure scenario for cemented THA stems [4].

The fatigue failure of hip prosthesis was reduced significantly in the past two decades [5,6]. However, every new implant design has to be checked against fatigue failure. In the literature, to simulate fatigue damage of implant, finite element models in association with cement damage algorithms have been used [7,8]. In a previous work [9], three-dimensional analysis of the mechanical interaction between a femoral stem and the femur in a hip arthroplasty was performed. In a related work [10], a quasi three dimensional finite element model for fatigue analysis of the hip implant was initially developed. The side-plate concept was introduced to account for the three-dimensional structural integrity of the cement and cortical bone and to recover the hoop stress in the cement mantle as membrane stress. This was achieved by an appropriate calibration of the geometric parameters. Two different damage rules; linear and non-linear were proposed to produce two different damage evolution algorithms for the estimation of the fatigue lifetime. In a subsequent work, the generated algorithm was implemented in the finite element code ABAQUS.

Some investigators have postulated that the failure mode of the bone-cement or bone-implant interface is a result of the shear stress distribution and shear strength of the interface. A fracture mechanics approach using strain energy density and stress intensity factors, combined with the assumption of an interface layer with gradual variation of physical properties, has also been used to describe interface failure modes. Such criteria can be used to define an objective function for the optimization problem [11]. Refs. [12–15] used theoretical optimization models to find the best overall external shape of the stem, by achieving similar shapes. Ref. [16] applied optimization methods to select the elastic modulus of the stem. Refs. [17,18], used a parallel walled hollow stem while [19,20] lessened the stiffness of the stem by using transverse holes.

In this study, an efficient, effective and automated design strategy is proposed to design a hip prosthesis. In this strategy, finite element analysis, Approximate model and a numerical optimization algorithm are integrated to create an automated design tool. Using this approach, shape design of the prosthesis is formulated in the form of an optimization problem that can be solved easily by a conventional numerical optimization algorithm. Computationally expensive objective and constraint functions in the optimization problem, which come from prosthesis dynamic finite element analysis results, are replaced with their approximations before the optimization problem is solved. Solution of the optimization problem leads to the optimum design.

2. Methods, geometric and finite element modeling

2.1. Methods

A shape or material design optimization problem can generally be formulated as a constrained minimization problem as [11].

minimize:

$$y_0(\mathbf{x}) \tag{1}$$

subjected to:

$$y_j(\mathbf{x}) \leqslant 0 \quad (j = 1, \ldots, n_c) \tag{2}$$

within the design space:

$$x_{il} \leqslant x_i \leqslant x_{iu} \quad (i = 1, \ldots, N) \tag{3}$$

where $y_0(\mathbf{x})$ is the objective function, $y_j(\mathbf{x})$ $(j = 1, \ldots, n_c)$ are the constraint functions and $\mathbf{x} = [x_1, x_2, \ldots, x_N]$ is the vector of design variables. x_{il} and x_{iu} describe the physical upper and lower bounds on design variables. n_c and N are the number of constraints and number of design variables, respectively. The constraint and objective functions may correspond to weight, penetration depth, energy absorption, etc.

Solution of Eqs. (1)–(3) for shape optimization problems can be efficiently done by replacing objective and constraint functions with their response surface (RS) approximations. Optimization with approximations is often referred to as approximate optimization in the literature. The approximate optimization method implemented in ANSYS DO module and used in this study is shown in Fig. 1. ANSYS DO module generates and utilizes polynomial RS approximation for objective or constraint function as following [21]

$$\tilde{y}(\mathbf{x}) = \underbrace{\underbrace{a_0 + \sum_{n=1}^{N} a_n x_{n\,linear} + \sum_{n=1}^{N} b_n x_{n\,quadratic}^2}_{quadratic} + \sum_{m=1}^{N-1}\sum_{n=m+1}^{N} c_{mn} x_m x_n}_{quadratic+crossterms} \tag{4}$$

where a, b, c are coefficients to be determined.

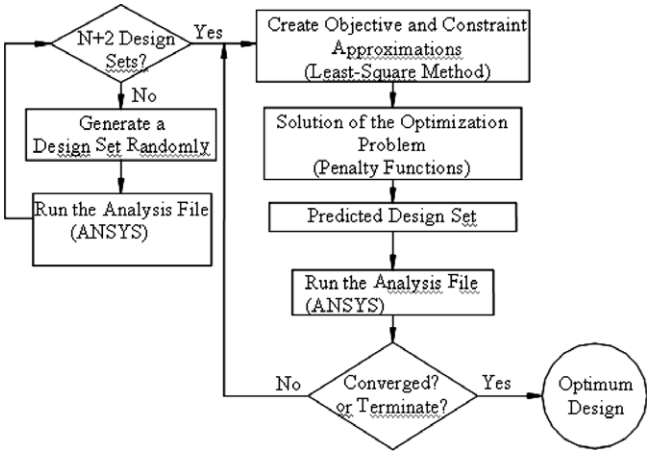

Fig. 1. Approximate design optimization process with ANSYS DO module.

Please cite this article in press as: Kayabasi O, Ekici B, The effects of static, dynamic and fatigue behavior on three-dimensional..., J Mater Design (2006), doi:10.1016/j.matdes.2006.08.012

In design optimization process, ANSYS DO first creates $N+2$ design sets to construct a linear approximation. Here "set" indicates values of all parameters for a specific design. ANSYS DO will either generate design sets randomly or use the existing ones in the optimization database. Shape optimization analysis is carried out at available design sets. Analysis results are then used to create linear approximations of the objective and constraints. Higher order approximations such as quadratic and quadratic with cross terms RS approximations are created using least square method when there are enough design sets in the database. The optimum design is predicted by solving Eqs. (1)–(3) with a numerical optimization algorithm based on penalty functions. The predicted optimum is verified by exact analysis (ANSYS). If the predicted objective and constraints are identical with the results from ANSYS, or the estimated optimum design is satisfactory enough, the optimization loop is stopped. Otherwise, the newly calculated results are added to the existing design sets and new approximations are created followed by the solution of the optimization problem.

2.2. Parametric and geometric modeling

Geometrical shapes have big influence on the performance of prosthesis. Those with smooth surfaces generally reduce stress concentrations and lead to high fatigue life of the prosthesis. Those with sharp or non-smooth surfaces provide good bonding capability at the interface and prevent possible sliding at the interface. The level of stress concentration and tendency for fatigue failure depend on the sharpness of the stem surfaces. In this study, a prosthesis geometry that will yield low stress values and high fatigue life is investigated. To achieve this goal, prosthesis is modeled parametrically using ANSYS parametric design language (APDL) [21]. The parameters used in the parametric model are referred to as design parameters and they are shown in Fig. 2. Best prosthesis shape (dimensions) is to be found by adjusting these parameters.

Fig. 2 also shows the antero-posterior side of the hip prosthesis along with the design parameters. In this figure, the proximal medial side of the prosthesis is represented by a circular arc. Design variables of $D_{(1)}, D_{(2)}, D_{(3)}, D_{(4)}, D_{(5)}, D_{(6)}, D_{(7)}$ and $D_{(10)}$ in Fig. 1 describe the geometry (dimensions) of the stem shape. The angle of the proximal medial side of the prosthesis with horizontal axis is represented by the design parameter of $D_{(9)}$ in Fig. 1. Design parameter of $D_{(8)}$ indicates the cement thickness between the prosthesis (stem shape) and for the bone. For smoother surface geometry, more design parameters must be chosen. The stem shape represents the lower part of the prosthesis that is inserted into the bone.

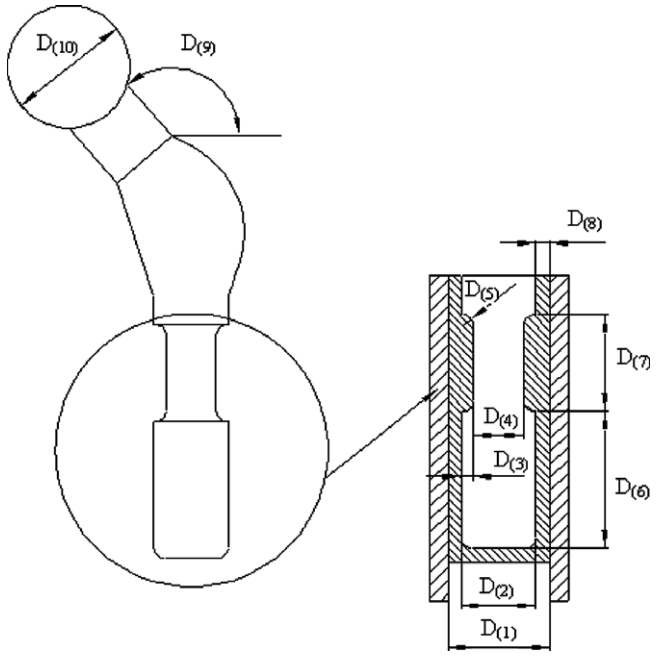

Fig. 2. Geometry of the hip prosthesis and design parameters selected.

It will be useful to remind the reader that more the number of design parameters the better the prosthesis shape (i.e. better performance) will be. However, the number of analysis (i.e. computational cost) needed in finding the best prosthesis design will be linearly or quadratically proportional with the number of design parameters selected.

Search process for best (optimum) prosthesis geometry or shape can be automated through a numerical optimization algorithm if the goal and the requirements are expressed in the form of an optimization problem definition as following: find *design parameters*:

$$D_{(1)}, D_{(2)}, D_{(3)}, D_{(4)}, D_{(5)}, D_{(6)}, D_{(7)}, D_{(8)}, D_{(9)} \text{ and } D_{(10)} \tag{5}$$

to minimize *design objective*:

$$\text{Maximum stress (von Mises stress)} \tag{6}$$

subjected to *design constraints*:

$$\sigma_{\text{stemshape}} \leqslant \sigma^{\text{Yield}}_{\text{stemshape}} \tag{7}$$

$$\sigma_{\text{cement}} \leqslant \sigma^{\text{Yield}}_{\text{cement}} \tag{8}$$

$$\sigma_{\text{femur}} \leqslant \sigma^{\text{Yield}}_{\text{femur}} \tag{9}$$

$$\tau_{\text{cement-femur}} \leqslant \tau^{\text{failure}}_{\text{cement-femur}} \tag{10}$$

$$\tau_{\text{cement-stemshape}} \leqslant \tau^{\text{failure}}_{\text{cement-stemshape}} \tag{11}$$

$$N_{\text{cement}} \geqslant 1 \tag{12}$$

within the *design space*:

$$18\text{ mm} \leqslant D_{(1)} \leqslant 20\text{ mm} \tag{13}$$

$$10\text{ mm} \leqslant D_{(2)} \leqslant 16\text{ mm} \tag{14}$$

$$0\text{ mm} \leqslant D_{(3)} \leqslant 3\text{ mm} \tag{15}$$

$$10\text{ mm} \leqslant D_{(4)} \leqslant 16\text{ mm} \tag{16}$$

$$0\text{ mm} \leqslant D_{(5)} \leqslant 3\text{ mm} \tag{17}$$

$$40\text{ mm} \leqslant D_{(6)} \leqslant 65\text{ mm} \tag{18}$$

$$20\text{ mm} \leqslant D_{(7)} \leqslant 40\text{ mm} \tag{19}$$

$$1\text{ mm} \leqslant D_{(8)} \leqslant 4\text{ mm} \tag{20}$$

$$120^\circ \leqslant D_{(9)} \leqslant 150^\circ \tag{21}$$

$$32\text{ mm} \leqslant D_{(10)} \leqslant 38\text{ mm} \tag{22}$$

Eq. (1) indicates design parameters describing the geometry/shape of the prosthesis. Eq. (2) represents design objective which is the minimization of the maximum stress on the whole prosthesis. Eqs. (3)–(8) correspond to design constraints on structural and fatigue strength limits on components of the prosthesis (i.e. stem shape, femur, cement, cement-femur interface, cement-stem shape interface). N_{cement} in Eq. (8) indicates fatigue safety factor for the bone-cement. Only fatigue safety of the bone-cement is considered in constraint definitions since cement is much more susceptible to fatigue failure than the prosthesis. Prosthesis geometry is generally assumed not to fail by fatigue. Eqs. (9)–(18) represent design space where parameters are to be searched. Limits of the design space are determined based on the experience and literature.

Objective and constraint functions in Eqs. (2)–(8) are not explicitly (analytically) known before the solution of the optimization problem. They are created applying the least-square fitting to finite element analysis results for certain number of randomly selected design parameter values that correspond to different prosthesis shapes. Since approximations of the objective and constraint functions are utilized, the optimization method is sometimes referred to as approximate optimization method and approximations are called as response surface approximations or response surface models. Linear and quadratic polynomial functions are often used to create the response surface approximations of the objective and constraint functions.

2.3. Finite element modeling

The first step is to build a FEM model corresponding to the geometric model. In this work, femur (cancellous bone, cortical shell), bone-cement and implant were meshed using four node tetrahedral elements. The mesh density gradually coarsens from the loading surface, which is potential

Please cite this article in press as: Kayabasi O, Ekici B, The effects of static, dynamic and fatigue behavior on three-dimensional..., J Mater Design (2006), doi:10.1016/j.matdes.2006.08.012

impact region, to the cancellous bone and from contact surface to outer surface. The complete model consisted of 72,458 elements: 48,205 for the femur, 13,760 for the bone-cement and 10,493 for the implant. All these were modeled with SOLID45 of ANSYS element library, defined by four nodes each having three degrees of freedom. The finite element models of the femur, the bone-cement and the implant are shown in Fig. 3.

The physical interactions among joints, which were involved in the prosthesis, were simulated by using contact-impact algorithms. The femur–bone-cement interface and the bone-cement–implant interface surface to surface contact-impact algorithms of ANSYS are used. These contact elements allow the introduction of intersurface friction. The femur and the bone-cement interface were modeled as a bonded contact type. Three different bone-cement and implant interface conditions were used.

1. Completely bonded contact type.
2. Debonded contact type with the coefficient of friction of $\mu = 0.22$.
3. Debonded contact type with the coefficient of friction of $\mu = 0$.

According to [22], the coefficient of friction of $\mu = 0.2$ was experimentally measured between 0.17 and 0.32 for polished or satin finish of the stem surface and the bone-cement material poly methyl methacrylate (PMMA).

The second step is to select material models. Two different material models for implant were used in the finite element simulation. These materials are Ti–6Al–4V and cobalt–chromium alloy. Behaviors of each of the two materials were represented by linear isotropic material model. Ti–6Al–4V had Young's modulus $E = 110$ GPa and Poisson's ratio $v = 0.316$ and cobalt–chromium had $E = 220$ GPa, $v = 0.3$ were assigned as homogeneous properties. The alternating stress versus number of cycles (S–N curve) for implant materials used in this study for fatigue calculations is given in the logarithmic scale in Fig. 4.

Cortical bone was considered as transversely isotropic ($E_x = E_y = 11.5$ GPa, $E_z = 17$ GPa; $G_{xy} = 3.6$ GPa, $G_{xz} = G_{yz} = 3.3$ GPa; $v_{xy} = 0.51$, $v_{xz} = v_{yz} = 0.31$ GPa) [23]. Cancellous bone was modeled as a linear isotropic material properties with $E = 2.13$ GPa and $v = 0.3$. Bone-cement (PMMA) was modeled as linear isotropic material properties with $E = 2.62$ GPa and $v = 0.3$. Viscoelastic behavior of bone-cement was modeled as a time hardening implicit creep equation of ANSYS material model library

$\acute{\varepsilon}_{cr} = 5.168 \times 10^{-6}\sigma^{1.858}t^{-0.717}$ [23,24].
$\acute{\varepsilon}_{cr}$ = The creep strain rate.
σ = Equivalent von Mises stress (MPa).
t = Time at end of substep (h).

The alternating stress versus number of cycles (S–N curve) for bone-cement used in this study for fatigue calculations is given in the logarithmic scale in Fig. 5.

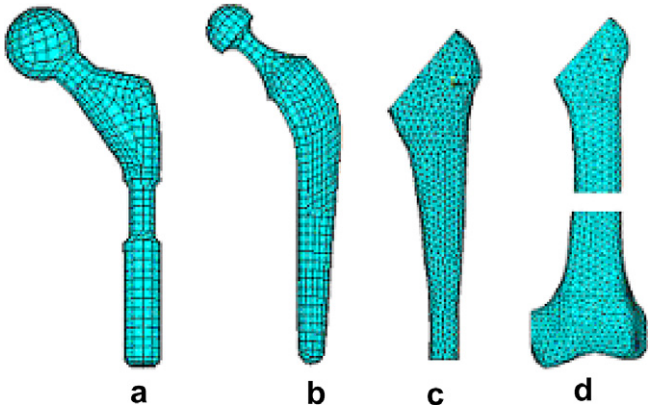

Fig. 3. Finite element model: (a) New design, (b) Charnley design, (c) bone-cement, (d) femur.

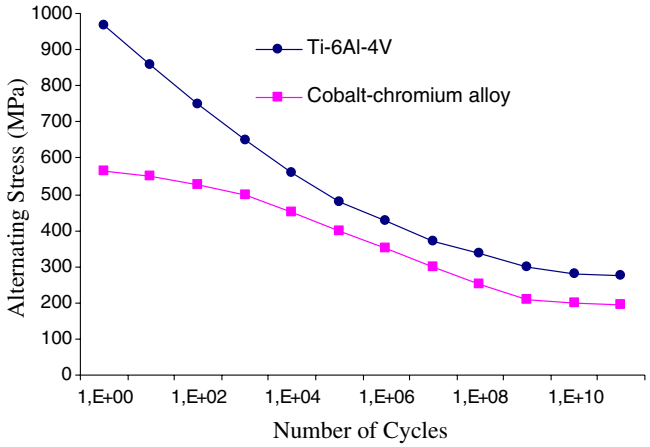

Fig. 4. Fatigue curves (S–N Curve) for Ti–6Al–4V and cobalt–chromium alloy materials.

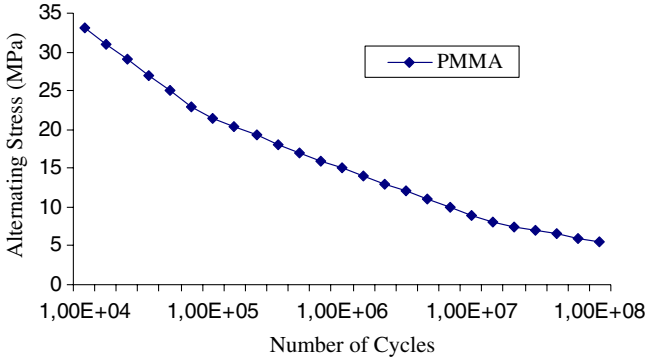

Fig. 5. Fatigue curves (S–N Curve) for bone-cement (PMMA).

A good implant design should satisfy maximum or an infinite fatigue life and reduce fatigue effects on bone-cement. This can only be ensured by physical testing or a fatigue analysis. In this study, fatigue life of the prosthesis upon finite element stress analysis is predicted using the computer code of ANSYS/Workbench [21]. Fatigue life of prosthesis is calculated based on Goodman, Soderberg, and Gerber fatigue theories which is illustrated in Table 1.

In Table 4, N indicates safety factor for fatigue life in loading cycle, S_e for endurance limit and S_u for ultimate tensile strength of the material. Mean stress σ_m and alternating stress σ_a are defined respectively, as

$$\sigma_m = \frac{(\sigma_{max} + \sigma_{min})}{2} \quad (23)$$

$$\sigma_a = \frac{(\sigma_{max} - \sigma_{min})}{2} \quad (24)$$

Von Misses stresses obtained from finite element analyses are utilized in fatigue life calculations. All fatigue analyses are performed according to infinite life criteria (i.e. $N = 10^9$ cycles).

The third step is to apply loading and boundary condition. Static and dynamic analyses of the prosthesis should be conducted to ensure about the safety of the design. In the literature, prostheses are often designed

Table 1
Fatigue theories and formulas used in fatigue life predictions

Fatigue theories	Fatigue formulas
Goodman	$\left(\frac{\sigma_a}{S_e}\right) + \left(\frac{\sigma_m}{S_u}\right) = \frac{1}{N}$
Soderberg	$\left(\frac{\sigma_a}{S_e}\right) + \left(\frac{\sigma_m}{S_y}\right) = \frac{1}{N}$
Gerber	$\left(\frac{N\sigma_a}{S_e}\right) + \left(\frac{N\sigma_m}{S_u}\right)^2 = 1$

according to the results of static analysis. Static finite element (FE) analyses are mostly conducted under body weight loads. However, dynamic effects may add up to about 10–20% or more loading to the prosthesis which must be taken into account so as to avoid fracture or fatigue failure. To investigate how static and dynamic analysis results differ from each other, the prosthesis was analyzed under both static body weight load and dynamic walking load.

For static analysis, a load of 3 kN (F_{static}) with an angle of 20° is applied on the surface of the implant bearing as shown in Fig. 3. Static load represents a person of 70 kg [25]. An abductor muscle load of 1.25 kN ($F_{abductor\ muscle}$) is applied at an angle of 20° to the proximal area of the greater trochanter. An ilio tibial-tract load of 250 N ($F_{ilio\ tibial\text{-}tract}$) is applied to the bottom of the femur in the longitudinal femur direction. The distal end of the femur is constrained not to move in horizontal direction.

For dynamic analysis, time-dependent walking load ($F_{dynamic}$) is applied as shown in Fig. 6. Time history of the dynamic load components for 5 s is demonstrated in Fig. 7 [26]. Finite element analyses of the prosthesis are carried out using ANSYS on a P4 2.0 GHz Intel processor PC. Each analysis takes about 26 h of CPU time.

3. Results

Optimization history graphics for stress values and design parameters using approximate optimization method are demonstrated in Figs. 8–11. Figs. 8 and 9 shows the change of the maximum stress on the hip prosthesis with iterations. Fig. 9 shows the change of the maximum stress on the bone-cement with iterations. Fig. 10 demonstrates the change of the design parameters of $D_{(1)}, D_{(2)}, D_{(3)}, D_{(4)}, D_{(5)}, D_{(6)}, D_{(7)}, D_{(8)}$ and $D_{(10)}$ with iterations and Fig. 11 demonstrates the change of the design parameter of D_9 with iterations. Optimum prosthesis geometry found after 50 optimization iterations is shown in Fig. 12. To reduce the computational cost, optimization process was limited with 50 iterations. More iteration may provide a better design. The optimum shape minimizes the stress values and maximizes the fatigue life of the prosthesis. From

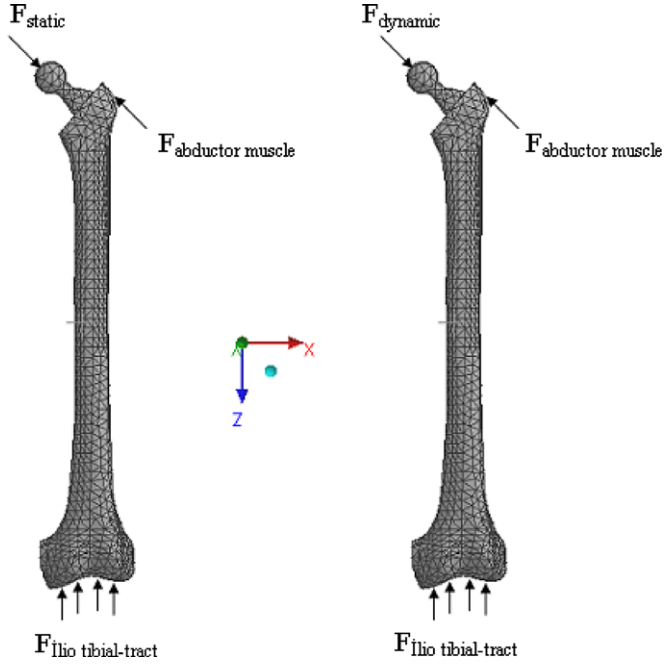

Fig. 6. Applied forces on the bone-cement-prosthesis assembly.

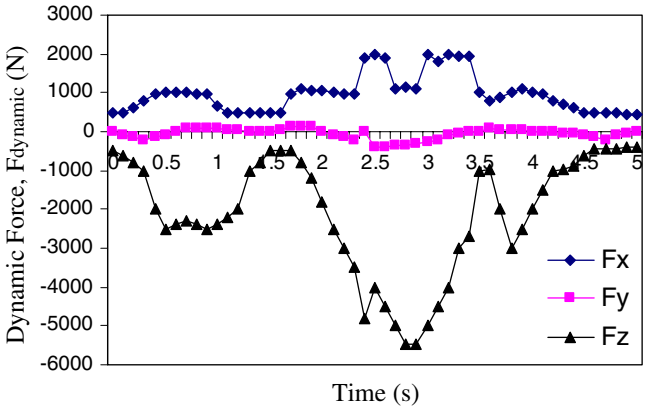

Fig. 7. Time history of walking load components on the prosthesis.

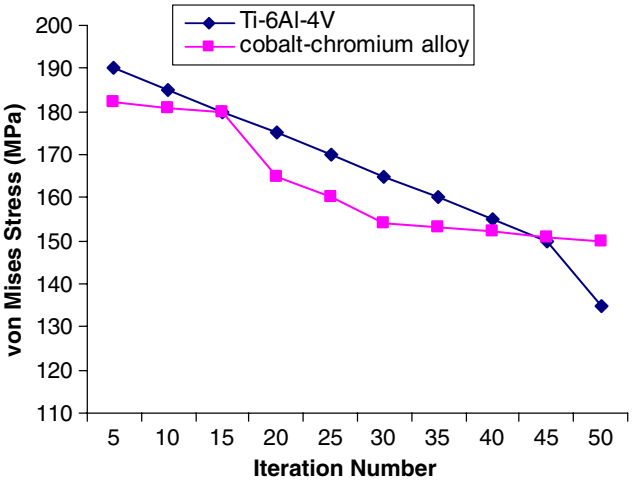

Fig. 8. The change of maximum stress on the hip prosthesis with iterations.

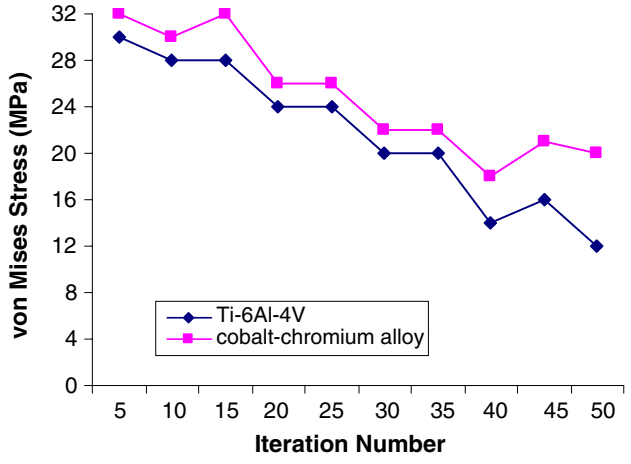

Fig. 9. The change of maximum stress on the bone-cement with iterations.

Fig. 12, it is seen that optimum stem shape has 128° angle of head.

The results obtained from simulations are outlined in this section. Fig. 13 shows the changes in Von Mises equivalent stress depending on changes in the angle of head

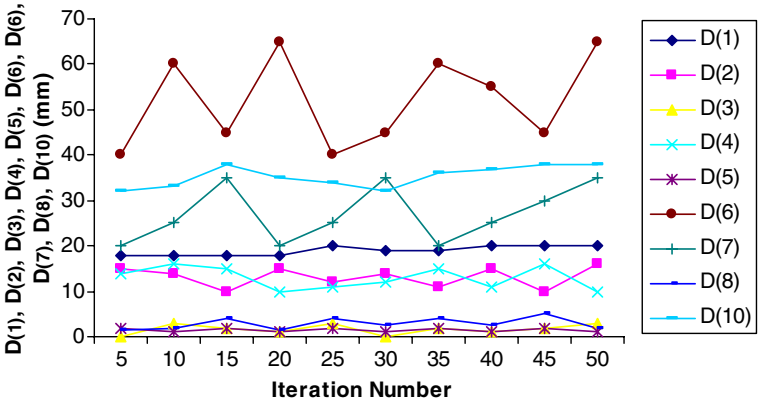

Fig. 10. The change of design parameters $D_{(1)}, D_{(2)}, D_{(3)}, D_{(4)}, D_{(5)}, D_{(6)}, D_{(7)}, D_{(8)}$ and $D_{(10)}$ with iterations.

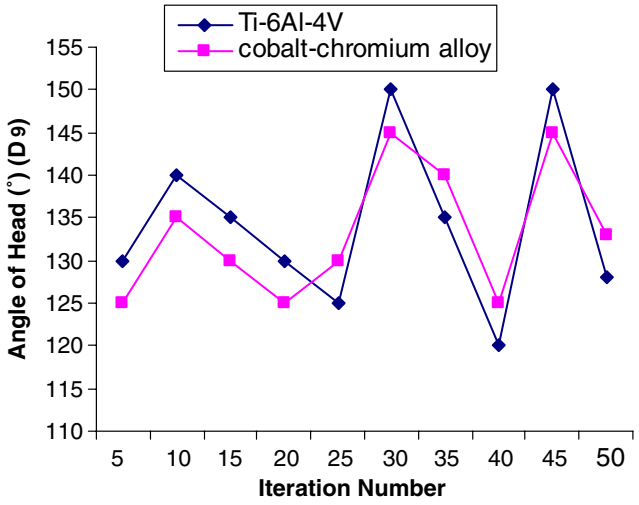

Fig. 11. The change of design parameter D_9 with iterations.

which is the first parameter studied in the optimization. From the figure it is easily seen that the minimum Von Mises stress was encountered between 125° and 130° . This angle range also shows the minimum Von Mises stress for Ti–6Al–4V alloy.

The stress that occurs on the prothesis is important for the sake of design accuracy. But the stress occurring on the bone-cement is much more critical. Fig. 14 shows the minimum Von Mises stress value for angles between 128° and 130°. The critical angle is found to be approximately 128° from the simulation results.

The Von Mises stress values must be also checked for Femur. The reason for that although prosthesis and cement could bear the stress due to applied loads, the femur might failed. In Fig. 15 the minimum stress value is 15 MPa for an angle of 130°.

The stress in the femur and cement are small with respect to the stress occurring on the prosthesis. In order to compare the results for the individual parts, a non-dimensional parameter must be used. This parameter is chosen as the stress/yield stress. As it is seen from Table 2 the ratio is the maximum for the cement. As expected the cement is most critical.

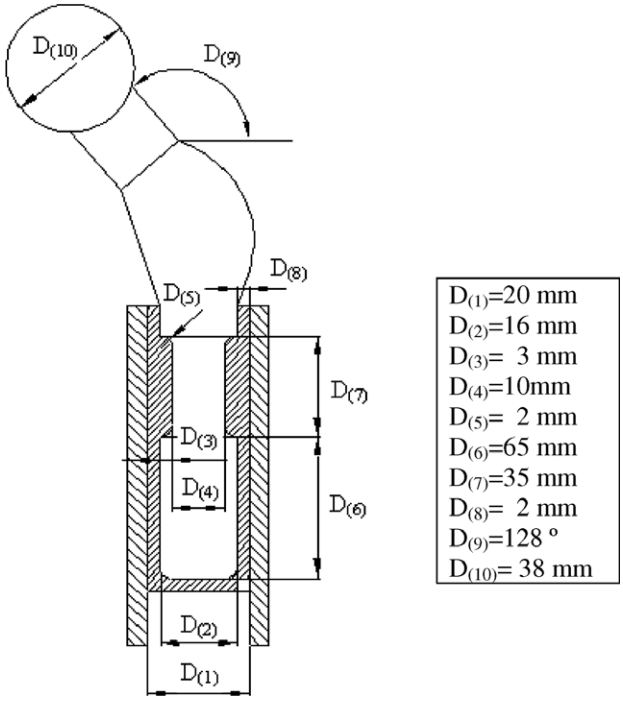

Fig. 12. Optimum prosthesis shape.

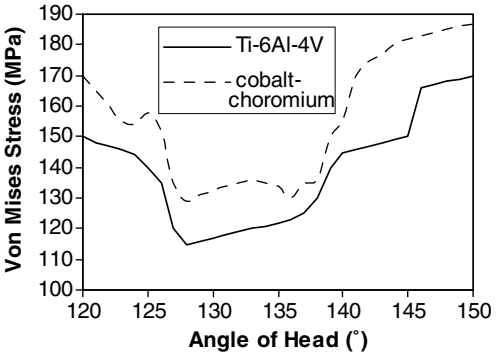

Fig. 13. Max Von Mises stress on hip prosthesis dependence to the changing angle of head.

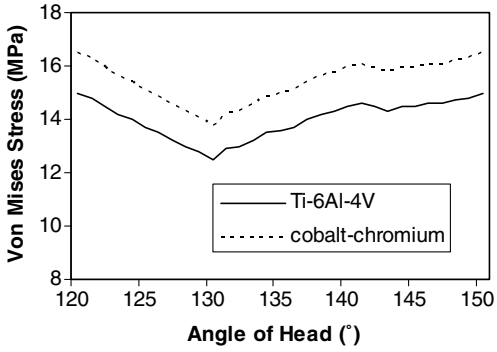

Fig. 14. Max Von Mises Stress on bone-cement dependence to the changing angle of head.

The durability of the prosthesis is compared for Ti–6Al–4V and for cobalt–chromium alloy. Fig. 16 predicts that since the safety factor is greater for Ti–6Al–4V than cobalt–chromium it is more durable.

One of the most important factors in the implant design is to reduce stress on bone-cement. If the stress is low, the fatigue life of bone-cement is long. Even through the hip prosthesis is durable, some of the implant designs increase bone-cement stress which may leads to cracking. In this study, investigate fatigue life of bone-cement Ti–6Al–4V and cobalt–chromium alloy were investigated. As seen from Fig. 17, Ti–6Al–4V is more durable for bone-cement than for cobalt–chromium.

Another important factor in implant design is stem-bone-cement interface. In this study stem-bone-cement interface conditions were used. The stem–bone-cement interface von Mises stress was greatest for the bonded stem and decreased with decreasing interface friction coefficient. That was greatest at 150° angle of head. Von Mises stress

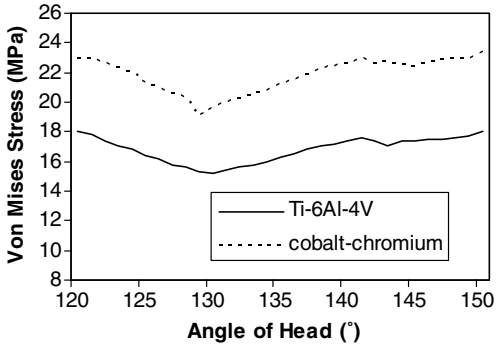

Fig. 15. Max Von Mises stress on femur dependence to the changing angle of head.

Table 2
Non-dimensional parameter

Component	Stress/yield stress
Hip prosthesis (Ti–6Al–4V)	0.135
Hip prosthesis (cobalt–chromium)	0.142
Bone-cement (Ti–6Al–4V)	0.216
Bone-cement (cobalt–chromium)	0.250
Femur (Ti–6Al–4V)	0.115
Femur (cobalt–chromium)	0.153

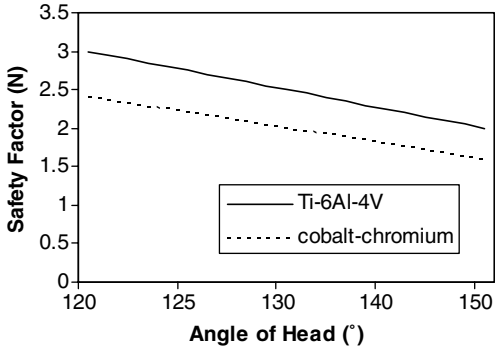

Fig. 16. Safety factors on hip prosthesis dependence to the changing angle of head.

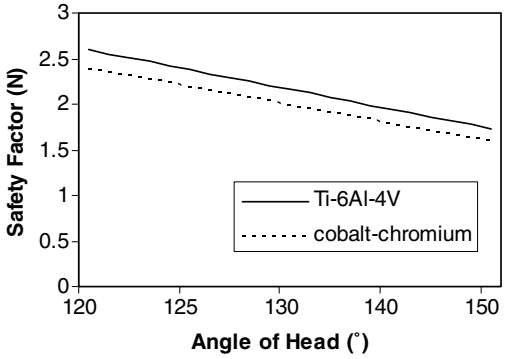

Fig. 17. Safety factors on bone-cement dependence to the changing angle of head.

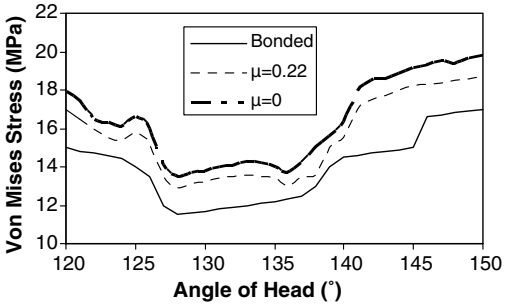

Fig. 18. Max Von Mises stress on bone-cement stem interface dependence to the changing angle of head with Ti–6Al–4V.

was also greatest for the frictionless case and smallest for the bonded case. Von Mises stress was significantly reduced on moving from 150° to 130° angle of head. At three stem-bone-cement interface condition, Ti–6Al–4V incurred less stress than cobalt–chromium alloy. These results are shown in Figs. 18 and 19.

Performance of the optimum prosthesis under dynamic loading with different friction coefficients at interfaces is compared with that of the commonly used Charnley type design in Table 3. Comparison is made for stresses as well as for the maximum displacement of the prosthesis at cement-stem shape interfaces. Optimum design found in this study is seen to yield less stress values (20–30% less)

Please cite this article in press as: Kayabasi O, Ekici B, The effects of static, dynamic and fatigue behavior on three-dimensional..., J Mater Design (2006), doi:10.1016/j.matdes.2006.08.012

Table 3
Compared results with Charnley design by static loading

	Optimum design (Ti–6Al–4V)	Optimum design (cobalt–chromium)	Charnley design (Ti–6Al–4V)
Von Mises stress (hip-prosthesis) (MPa)	112	130	138
Von Mises stress (bone-cement) (MPa)	12.3	14	16
Von Mises stress (femur) (MPa)	15.3	19.2	22
Von Mises stress (bone-cement–stem interface) bonded (MPa)	11.5	13.6	15.2
Von Mises stress (bone-cement–stem interface) $\mu = 0$ (MPa)	13.5	17.3	18.3
Von Mises stress (bone-cement–stem interface) $\mu = 0.22$ (MPa)	12.9	15.8	17.6
Safety factors (hip prosthesis) (N)	2.7	2.2	1.9
Safety factors (bone-cement) (N)	2.5	2.3	1.8
Displacement (bone-cement–stem interface) (mm)	0.035	0.051	0.087

than Charnley type prosthesis design. It also moves less than Charnley type design in the bone-cement thus providing more fixation.

4. Conclusion

This study shows that optimization techniques and different material models can be combined with fully 3-D stress analysis model to obtain femoral component designs that are optimized in the sense of reducing and smoothing stresses adjacent to the interface. Both objective functions based on interface failure and remodeling potential were improved using bone-cement locking as design variables.

Static and dynamic FE analyses of stems were conducted using ANSYS. Based on static and dynamic FE analysis results, safety factors for fatigue life were calculated. Fatigue calculations were carried out for Ti–6Al–4V and cobalt–chromium alloy materials based on Goodman, Soderberg, and Gerber fatigue theories. All calculations aim at infinite fatigue life criteria. The best stem shape for fatigue under static loading is found to be fabricated of Ti–6Al–4V material. This is also the best one under dynamic loading. However, safety factors differ under static and dynamic loading conditions. This indicates that stem shapes predicted to be safe against fatigue under static loading may fail under dynamic repetitive loadings.

Results of this study showed a state of stress at the stem–cement interface indicative of locking geometry for the debonded stem ($\mu = 0$ and 0.22) that was attributed to the stem locking geometry at the medial interface. The stem–cement interface friction was found to play a major role in the magnitudes and orientations of stress at the interface and within the cement mantle. The normal stress at the stem–cement interface decreased with friction where as shear stress increased. In addition, the cement stress was larger for debonded stems than bonded stems, and the magnitude of the stress in general decreased with increasing friction coefficient. In accordance with the hypothesis of this study, the major effect of bone-cement creep was stress relaxation and stem subsidence. The effect was more pronounced for debonded stems wherever interface stress was larger.

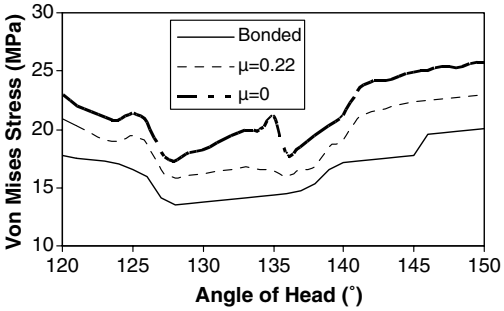

Fig. 19. Max Von Mises stress on bone-cement stem interface dependence to the changing angle of head with cobalt–chromium.

The optimum shape results have better behavioral characteristic than Charnly shapes. A general conclusion is that implant hip prostheses can be designed and studied with computer models before implementation on the patient. This procedure reduces design time while helping to prevent permanent damage caused by miss-implementation.

References

[1] Carter DR, Beaupr'e GS. Skeletal function and form. Cambridge, United Kingdom: Cambridge University Press; 2001.
[2] Brekelmans WAM, Poort HW, Sloof TJJH. A new method to analyse the mechanical behavior of skeletal parts. Acta Orthop Scand 1972;43:301–17.
[3] Harrigan TP, Harris WH. A three-dimensional non-linear finite element study of the effect of cement-prosthesis debonding in cemented femoral total hip components. J Biomech 1991;24:1047–58.
[4] Jasty M, Malone WJ, Bragdon CR, O'Connor D, Haire T, Harris WH. The initiation of failure in cemented femoral components of hip arthroplasties. J Bone Joint Surg 1991;73B:551–8.
[5] Sotereanos NG, Engh CA, Glassman AH, Macalino GE. Cementless femoral components should be made from cobalt chrome. Clin Orthop 1995;313:146–53.
[6] Wroblewski BM, Sidney PD. Charnley low friction arthroplasty of the hip. Long term result. Clin Orthop 1993;292:191–201.
[7] Verdonschot N, Huiskes R. The effects of cement–stem debonding in THA on the long-term failure probability of cement. J Biomech 1997;30:795–802.
[8] Dolinski K. Fatigue reliability assessment of cemented hip prosthesis. J Theor Appl Mech 1999;3:505–18.
[9] Penza E, Poles G. Analisi Tridimensionale dell'Interazione Meccanica Femore-Protesi in una Endoprotesi d'Anca. Master thesis, Technical University of Milan;1998 [in Italian].

Please cite this article in press as: Kayabasi O, Ekici B, The effects of static, dynamic and fatigue behavior on three-dimensional..., J Mater Design (2006), doi:10.1016/j.matdes.2006.08.012

[10] Colombi P. Fatigue analysis of cemented hip prosthesis: model definition and damage evolution algorithms. Int J Fatigue 2002;24:895–901.
[11] Katoozian H. Three dimensional design optimization of femoral components of total hip endoprostheses. Ph.D. dissertation. Cleveland (OH): Case Western Reserve University; 1993.
[12] Katoozian, H., Davy, D.T., 1993. Three-dimensional shape optimization of femoral components of total hip prostheses. In: Bioengineering Conference, BED-vol. 24. ASME; p. 552–5.
[13] Huiskes R, Boeklagen R. Mathematical shape optimization of hip prosthesis design. J Biomech 1989;22:793–804.
[14] Yoon YS, Jang GH, Kim YY. Shape optimal design of the stem of a cemented hip prosthesis to minimize stress concentration in the cement layer. J Biomech 1989;22:1279–84.
[15] Hedia HS, Barton DC, Fisher J, Elmidany TT. A method for shape optimizations of a hip prosthesis to maximizes the fatigue life of the cement. Med Eng Phys 1996;18:647–54.
[16] Kuiper JH. Numerical optimization of artificial hip joint designs. Ph.D. Thesis, Nijmegen, Holland, University of Nijmegen; 1993.
[17] Bobyn JD, Glassman AH, Goto H, Krygier JJ, Miller JE, Brooks CE. The effect of stem stiffness on femoral bone resorbtion after canine porous coated total hip replacement. Clinic Orthopaedics Related Res 1990;261:196–213.
[18] Bobyn JD, Glassman AH, Goto H, Krygier JJ, Miller JE, Brooks CE. The effect of stem stiffness on femoral bone resorbtion after canine porous coated total hip replacement. Clinic Orthopaedics Related Res 1990;261:196–213.
[19] Engelhardt JA, Saha S. Effect of femoral component section modulus on the stress distribution in the proximal human femur. Med Biol Eng Comp 1988;26:38–45.
[20] Viceconti M, Toni A, Giunti A. Effects of some technological aspects on the fatigue strength of a cementless hip stem. J Biomed Mater Res 1995;29:875–81.
[21] ANSYS., 2003. Ansys Theory Reference Manual, Release 8.0 Ansys Inc.
[22] Nuno N, Amabili M, Groppeti R, Rossi A. Static coefficient of friction between Ti–6Al–4V and PMMA used in cemented hip and knee implants. J Biomed Mater Res 2002;59:191–200.
[23] Norman TL, Thyagarajan G, Saligrama VC, Gruen TA, Blaha JD. Stem surface roughness alters creep induced subsidence and 'taper-lock' in a cemented femoral hip prosthesis. J Biomech 2001;34:1325–33.
[24] Chwirut JD. Long term compressive creep deformation and damage in acrylic bone cements. J Biomed Mater Res 1984;18:25–37.
[25] El-Sheikh HF, J MacDonalds B, Hashmi MSJ. Material selection in the design of the femoral component of cemented total hip replacement. J Mater Process Technol 2002;122:309–17.
[26] Bergmann G, Graichen F, Rohlmann A. Hip joint loading during walking and running, measured in two patients. J Biomech 1993;26:969–90.

Please cite this article in press as: Kayabasi O, Ekici B, The effects of static, dynamic and fatigue behavior on three-dimensional..., J Mater Design (2006), doi:10.1016/j.matdes.2006.08.012